ORIGINAL SCIENTIFIC PAPER

CROATICA CHEMICA ACTA

Croat. Chem. Acta **2026**, *99*(3)
Published online: November 20, 2026
DOI: 10.5562/cca4375

HKD 1926

Synthesis, Characterization and Biological Evaluation of Benzimidazole-Chalcones as Potent Anti-Breast Cancer Agents

Nagesh V. Edake,[1] Dnyaneshwar M. Sirsat,[2] Samadhan A. Shenmare,[3] Sadanand N. Shringare,[1] Nikita N. Mali,[4] Raghunath B. Bhosale,[1] Pravin S. Bhale[3,*]

[1] Organic Chemistry Research Laboratory, School of Chemical Sciences, Punyashlok Ahilyadevi Holkar Solapur University, Solapur-413 255, Maharashtra, India
[2] Department of Chemistry, Anandibai Raorane Arts, Commerce & Science College, Vaibhavwadi, Dist-Sindhudurg-416 810, Maharashtra, India
[3] Department of Chemistry, Yeshwantrao Chavan Mahavidyalaya, Tuljapur, Dist-Dharashiv-413 601, Maharashtra, India
[4] Department of Chemistry, Sub-Campus, Dr. Babasaheb Ambedkar Marathwada University, Dharashiv-413 501, Maharashtra, India
* Corresponding author's e-mail address: bhale.ps@gmail.com

RECEIVED: July 5, 2026 * REVISED: October 4, 2026 * ACCEPTED: October 5, 2026

Abstract: A novel series of benzimidazole–chalcone derivatives (**6a**–**k**) were synthesized and evaluated for their *in vitro* anticancer potential against human breast cancer cells and normal Vero cells. The target compounds were prepared *via* a base-catalyzed aldol condensation of 2-acetylbenzimidazole with various fluoro- and trifluoromethyl-substituted aromatic aldehydes under mild reaction conditions. The key intermediate, 2-acetylbenzimidazole, was obtained through condensation of *o*-phenylenediamine or 4-methylbenzene-1,2-diamine with lactic acid followed by oxidation of the resulting hydroxyl intermediate. The anticancer activity of the synthesized benzimidazole–chalcones was assessed against the estrogen receptor–positive human breast cancer cell line MCF-7 using the sulforhodamine B (SRB) assay, while their cytotoxicity toward normal Vero cells was evaluated to assess preliminary selectivity. The compounds exhibited a broad spectrum of anticancer activity, with GI_{50} values ranging from low µM to inactive levels. Notably, fluoro-substituted derivatives displayed enhanced activity, with the difluoro analogue (*E*)-1-(1H-benzo[d]imidazol-2-yl)-3-(3,5-difluorophenyl)prop-2-en-1-one (**6f**) emerging as the most potent compound (GI_{50} = 3.66 µM), while derivatives bearing bulky trifluoromethyl substituents showed reduced or negligible activity. Against Vero cells, most derivatives displayed relatively weak growth inhibition, while selected compounds showed moderate activity. The comparatively higher GI_{50} values against Vero cells than MCF-7 cells for several derivatives suggest preliminary cancer-cell selectivity. Structure–activity relationship analysis revealed that both the nature and position of substituents significantly influence anticancer efficacy. Although less potent than adriamycin, several derivatives demonstrated promising cytostatic effects, highlighting the benzimidazole–chalcone scaffold as a valuable platform for further optimization and mechanistic exploration toward the development of improved anti-breast cancer agents.

Keywords: benzimidazole, chalcone, aldol condensation, anti-cancer activity.

INTRODUCTION

CANCER continues to represent a major global public health burden and remains one of the leading causes of mortality worldwide. According to the World Health Organization (WHO), nearly 10 million cancer-related deaths were reported in 2020, while approximately 20 million new cases and 9.7 million deaths were documented globally in 2022, with projections indicating a 77 % increase in incidence by 2050.[1–4] Among all malignancies, breast cancer is the most frequently diagnosed cancer in women and a principal contributor to cancer-associated mortality. Although advancements in early detection and therapeutic strategies have significantly improved patient outcomes, major clinical challenges such as drug resistance, lack of selectivity, systemic toxicity, and disease recurrence continue to limit the long-term effectiveness of current chemotherapeutic regimens. These limitations highlight the pressing need for the development of novel, more selective, and mechanistically diverse anticancer agents with improved therapeutic indices.[5,6]

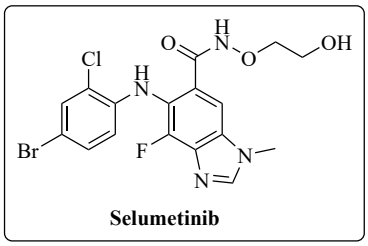
This work is licensed under a Creative Commons Attribution 4.0 International License.

In this context, heterocyclic compounds have emerged as privileged scaffolds in medicinal chemistry due to their structural diversity, pharmacophoric richness, and ability to interact with multiple biological targets. Among them, the benzimidazole nucleus has gained particular attention because of its structural similarity to purine bases, enabling effective interactions with nucleic acids and enzyme active sites. Benzimidazole derivatives have been extensively reported to exhibit a wide range of pharmacological activities, including antibacterial,[7,8] anti-tubercular,[9,10] antifungal,[11] antimicrobial,[9,11] antiprotozoal,[12,13] anti-HIV,[14] and antiviral activities,[15] and show potential as protein kinase inhibitors.[16] Notably, several benzimidazole-based compounds have demonstrated significant antiproliferative effects against human breast cancer cell lines such as MCF-7 and MDA-MB-231, acting through mechanisms that include inhibition of tubulin polymerization, DNA intercalation, and modulation of apoptosis-related pathways.[17–19] These findings establish benzimidazole as a promising core scaffold for the rational design of next-generation anticancer agents.

Parallel to this, chalcones defined by their α,β-unsaturated carbonyl framework connecting two aromatic systems have attracted considerable interest due to their broad spectrum of biological activities, particularly in cancer chemotherapy. Chalcone derivatives have been shown to exert cytotoxic effects against a variety of tumor cell lines by inducing apoptosis, causing cell cycle arrest, inhibiting angiogenesis, and suppressing key molecular targets such as NF-κB, PI3K/Akt, and tubulin.[20,21] The structural simplicity and synthetic flexibility of chalcones allow for facile chemical modification, enabling systematic structure–activity relationship (SAR) studies to optimize anticancer potency and selectivity.

Building upon the complementary pharmacological profiles of these two scaffolds, the molecular hybridization approach has emerged as a powerful strategy to design multifunctional anticancer agents. The conjugation of benzimidazole and chalcone moieties into a single molecular framework is anticipated to produce synergistic effects by combining multiple modes of action within one entity.[22] Recent studies have reported that benzimidazole–chalcone hybrids exhibit enhanced antiproliferative activity and improved selectivity toward cancer cells when compared to their individual parent scaffolds or standard chemotherapeutic agents.[23] These hybrid molecules have been proposed to act through diverse mechanisms, including topoisomerase inhibition, mitochondrial pathway-mediated apoptosis, reactive oxygen species (ROS) generation, and disruption of cancer-related signaling cascades, underscoring their potential as multi-target-directed ligands.[25]

Several benzimidazole-containing drugs have been approved for diverse therapeutic applications, highlighting



Selumetinib

Figure 1. Benzimidazole-containing marketed anticancer drug.

the clinical significance of the benzimidazole scaffold. In oncology, selumetinib, a MEK inhibitor, is used to treat NF1-associated inoperable plexiform neurofibromas, while vismodegib, a hedgehog pathway inhibitor, is indicated for advanced basal cell carcinoma. The clinical success of Selumetinib (Figure 1) demonstrates that the benzimidazole nucleus is a drug-like, biologically compatible, and therapeutically powerful scaffold.[26] This strongly supports the rationale for developing benzimidazole–chalcone hybrids, where the benzimidazole core provides validated anticancer relevance and the chalcone moiety contributes tunable cytotoxic and multi-target activity potentially leading to compounds with enhanced selectivity, reduced resistance, and improved therapeutic profiles in breast cancer.

Despite these promising advances, systematic investigations into the structure–activity relationships, molecular mechanisms, and breast cancer-specific efficacy of newly designed benzimidazole–chalcone derivatives remain limited. In particular, there is a growing need to develop novel analogues with improved cytotoxic selectivity, reduced off-target effects, and enhanced activity against resistant breast cancer phenotypes. Building upon these findings and continuing our efforts toward the development of novel bioactive anticancer agents,[27–31] the present study focuses on the rational synthesis, comprehensive structural characterization, and *in vitro* biological evaluation of a new series of benzimidazole–chalcone derivatives (**6a**–**k**) as potential anti-breast cancer agents. This work aims to identify lead candidates with promising therapeutic profiles and to contribute to the ongoing development of effective and selective chemotherapeutic strategies for breast cancer management.

EXPERIMENTAL

Materials and Methods

All chemicals and reagents employed in the synthesis were of analytical grade and procured from commercial suppliers without further purification. Reaction progress was monitored by thin-layer chromatography (TLC) using silica gel 60 F_{254} aluminum-backed plates (Merck), with visualization

under ultraviolet light and/or iodine vapor. All solvents were dried using appropriate drying agents prior to use. The melting points of the synthesized compounds were determined by the open-end capillary method using a digital melting point apparatus and are reported without correction. ^{1}H NMR spectra were recorded in $CDCl_3$ on a Bruker AV-400 MHz spectrometer, while ^{13}C NMR spectra were acquired at 75 MHz. Chemical shifts (δ, ppm) are reported relative to tetramethylsilane (TMS) as an internal standard. Infrared (IR) spectra were recorded on a Shimadzu FT-IR spectrophotometer using 1 % potassium bromide (KBr) pellets. High-resolution mass spectra (HRMS) were recorded at SAIF, Panjab University, Chandigarh, using a Thermo Scientific Q Exactive Plus Biopharma Orbitrap mass spectrometer (Thermo Fisher Scientific, USA) with ESI in positive-ion mode. All synthesized compounds **6a**–**k** were purified by column chromatography followed by recrystallization from ethanol and were obtained with a purity of > 95 %, as confirmed by the available spectroscopic and mass-spectrometric characterization data. *In vitro* anticancer activity studies were carried out at the Tata Memorial Centre, Advanced Centre for Treatment, Research and Education in Cancer (ACTREC), Kharghar, Navi Mumbai–410210.

Synthesis

GENERAL PROCEDURE FOR THE PREPARATION OF BENZIMIDAZOLE CHALCONES (4a–k)

2-Acetylbenzimidazole **4** (1.0 mmol) was dissolved in PEG-300 (10 mL), and the appropriate fluoro- or trifluoromethyl-substituted aromatic aldehyde **5** (1.0 mmol) was added. To this mixture, 10 % (*w*/*v*) aqueous potassium hydroxide solution was added dropwise. The reaction mixture was stirred at 50–60 °C for 18 h. Reaction progress was monitored by thin-layer chromatography (TLC). Upon completion, the mixture was allowed to cool to room temperature and then poured into ice-cold water. The solution was neutralized with glacial acetic acid, resulting in the formation of a precipitate. Purification by column chromatography and recrystallization from ethanol yielded benzimidazole chalcones **6a**–**k** as yellow crystalline solids.

SPECTRAL DATA OF REPRESENTATIVE COMPOUNDS

(*E*)-1-(1*H*-benzo[*d*]imidazol-2-yl)-3-phenylprop-2-en-1-one (6a)

Yellow solid; 94 %; 202–204 °C; IR (cm^{-1}): 3251 (NH), 1662 (C=O), 1595 (C=C); ^{1}H NMR ($CDCl_3$, 400 MHz): δ = 10.72 (Broad s, 1H, NH), 8.22 (d, *J* = 15.6 Hz, 1H, –CH=CH–), 8.05 (d, *J* = 15.6 Hz, 1H, –CH=CH–), 7.79–7.78 (m, 4H), 7.53–7.44 (m, 5H); ^{13}C NMR ($CDCl_3$, 75 MHz): δ = 181.7, 147.7, 139.2, 137.2, 129.7, 129.6, 128.0, 127.2, 125.1, 118.2, 115.2; HRMS: Calcd for $C_{16}H_{12}N_2O$ Exact mass: 248.095, found (ESI M+H) HRMS: *m* / *z* 249.0540 (M+H).

(*E*)-1-(1*H*-benzo[*d*]imidazol-2-yl)-3-(2-fluorophenyl)prop-2-en-1-one (6b)

Yellow solid; 90 %; 210–212 °C; IR (cm^{-1}): 3267 (NH), 1662 (C=O), 1599 (C=C); ^{1}H NMR ($CDCl_3$, 400 MHz): δ = 10.42 (Broad s, 1H, NH), 8.24 (m, 1H), 7.89–7.87 (m, 2H), 7.44–7.42 (m, 3H), 7.26–7.13 (m, 4H); ^{13}C NMR ($CDCl_3$, 75 MHz): δ = 181.3, 154.3, 143.9, 133.8, 131.7, 130.9, 125.9, 124.3, 122.0, 120.3, 116.6, 116.2, 112.3; HRMS: Calcd for $C_{16}H_{11}FN_2O$; Exact mass: 266.0855, found (ESI M+H) HRMS: *m* / *z* 267.0968 (M+H).

(*E*)-1-(1*H*-benzo[*d*]imidazol-2-yl)-3-(2,4-difluorophenyl)prop-2-en-1-one (6c)

Yellow solid; 94 %; 226–228 °C; IR (cm^{-1}): 3270 (NH), 1660 (C=O), 1599 (C=C); ^{1}H NMR ($CDCl_3$, 400 MHz): δ = 10.70 (Broad s, 1H, NH), 8.10–8.00 (m, 1H), 7.97–7.95 (m, 1H), 7.78–7.74 (m, 2H), 7.59 (d, *J* = 8.0 Hz, 1H), 7.47–7.38 (m, 2H), 7.15–7.11 (m, 2H); ^{13}C NMR ($CDCl_3$, 75 MHz): δ = 181.4, 159.2, 151.7, 141.6, 138.7, 134.4, 129.2, 125.1, 121.0, 117.3, 115.3, 12.0, 110.2; HRMS: Calcd for $C_{16}H_{10}F_2N_2O$; Exact mass: 284.0761, found (ESI M+H) HRMS: *m* / *z* 285.0432 (M+H).

(*E*)-3-(4-fluorophenyl)-1-(5-methyl-1*H*-benzo[*d*]imidazol-2-yl)prop-2-en-1-one (6d)

Yellow solid; 87 %; 200–202 °C; IR (cm^{-1}): 3277 (NH), 1663 (C=O), 1599 (C=C); ^{1}H NMR ($CDCl_3$, 400 MHz): δ = 10.44 (Broad s, 1H, NH), 8.08–7.99 (m, 2H), 7.83 (d, *J* = 8.4 Hz, 1H), 7.77–7.73 (m, 2H), 7.35 (s, 1H), 7.22 (d, *J* = 8.4 Hz, 1H), 7.16–7.10 (m, 2H), 2.52 (s, 3H, –CH_3); ^{13}C NMR ($CDCl_3$, 75 MHz): δ = 181.3, 163.4, 148.7, 144.5, 133.8, 131.2, 131.1, 126.5, 123.9, 121.9, 120.6, 116.3, 116.1, 112.2, 29.5; HRMS: Calcd for $C_{17}H_{13}FN_2O$; Exact mass: 280.1012, found (ESI M+H) HRMS: *m* / *z*: 281.1176 (M+H).

(E)-1-(5-chloro-1H-benzo[d]imidazol-2-yl)-3-(4-fluorophenyl)prop-2-en-1-one (6e)

Yellow solid; 92 %; 232–234 °C; IR (cm^{-1}): 3167 (NH), 1660 (C=O), 1599 (C=C); ^{1}H NMR ($CDCl_3$, 400 MHz): δ = 10.33 (Broad s, 1H, NH), 8.02 (d, *J* = 8.4 Hz, 1H), 7.92 (d, *J* = 12.8 Hz, 1H), 7.84–7.79 (m, 2H), 7.62 (d, *J* = 12.8 Hz, 1H), 7.31–7.14 (m, 2H), 7.11–6.98 (m, 2H); ^{13}C NMR ($CDCl_3$, 75 MHz): δ = 181.9, 156.0, 142.1, 136.2, 132.7, 131.3, 126.2, 124.4, 122.0, 121.7, 118.5, 115.2, 115.0, 114.5; HRMS: Calcd for $C_{16}H_{10}ClFN_2O$; Exact mass: 300.0466, found (ESI M+H) HRMS: *m* / *z* 301.0101 (M+H).

(*E*)-1-(1*H*-benzo[*d*]imidazol-2-yl)-3-(3,5-difluorophenyl)prop-2-en-1-one (6f)

Yellow solid; 90 %; 240–242 °C; IR (cm^{-1}): 3069 (NH), 1665 (C=O), 1585 (C=C); ^{1}H NMR ($CDCl_3$, 400 MHz): δ = 10.44 (Broad s, 1H, NH), 8.11 (d, *J* = 16.0 Hz, 1H, –CH=CH–), 7.96–

7.92 (m, 2H), 7.59–7.53 (m, 1H), 7.44–7.32 (m, 2H), 7.30–7.25 (m, 1H), 6.93–6.87 (m, 2H); ^{13}C NMR ($CDCl_3$, 75 MHz): δ = 181.9, 159.8, 147.7, 139.2, 137.2, 132.4, 129.6, 129.4, 125.3, 115.2, 114.4; HRMS: Calcd for $C_{16}H_{10}F_2N_2O$; Exact mass: 284.0761, found (ESI M+H) HRMS: 285.0421 (M+H).

(*E*)-3-(3,5-difluorophenyl)-1-(5-methyl-1*H*-benzo[*d*]imidazol-2-yl)prop-2-en-1-one (6g)

Yellow solid; 94 %; 254–256 °C; IR (cm^{-1}): 3283 (NH), 1660 (C=O), 1586 (C=C); ^{1}H NMR ($CDCl_3$, 400 MHz): δ = 10.48 (Broad s, 1H, NH), 8.08 (d, *J* = 15.2 Hz, 1H, –CH=CH–), 7.91–7.71 (m, 2H), 7.52–7.32 (m, 1H), 7.12–6.96 (m, 2H), 6.89–6.73 (m, 2H), 2.51 (s, 3H, –CH_3); ^{13}C NMR ($CDCl_3$, 75 MHz): δ = 181.6, 155.2, 143.8, 140.1, 136.0, 134.7, 133.5, 128.6, 125.2, 122.4, 117.2, 115.9, 115.1, 114.5, 26.8; HRMS: Calcd for $C_{17}H_{12}F_2N_2O$; Exact mass: 298.0918, found (ESI M+H) HRMS: *m* / *z* 299.1075 (M+H).

(*E*)-1-(5-chloro-1*H*-benzo[*d*]imidazol-2-yl)-3-(3,5-difluorophenyl)prop-2-en-1-one (6h)

Yellow solid; 90 %; 248–250 °C; IR (cm^{-1}): 3255 (NH), 1665 (C=O), 1600 (C=C); ^{1}H NMR ($CDCl_3$, 400 MHz): δ = 10.29 (Broad s, 1H, NH), 8.13 (d, *J* = 15.4 Hz, 1H, –CH=CH–), 7.88–7.75 (m, 2H), 7.49–7.30 (m, 1H), 7.18–6.99 (m, 2H), 6.69–6.60 (m, 2H); ^{13}C NMR ($CDCl_3$, 75 MHz): δ = 181.9, 159.9, 146.4, 135.1, 132.7, 132.6, 131.7, 130.7, 129.2, 129.1, 126.9, 122.7, 117.9, 117.7; HRMS: Calcd for $C_{16}H_9ClF_2N_2O$; Exact mass: 318.0371, found (ESI M+H) HRMS: *m* / *z* 319.0506 (M+H).

(*E*)-1-(1*H*-benzo[*d*]imidazol-2-yl)-3-(4-(trifluoromethyl)phenyl)prop-2-en-1-one (6i)

Yellow solid; 88 %; 262–264 °C; IR (cm^{-1}): 3281 (NH), 1666 (C=O), 1606 (C=C); ^{1}H NMR ($CDCl_3$, 400 MHz): δ = 10.57 (Broad s, 1H, NH), 8.20 (d, *J* = 16.0 Hz, 1H, –CH=CH–), 8.06 (d, *J* = 16.0 Hz, 1H, –CH=CH–), 7.97 (d, *J* = 7.6 Hz, 1H), 7.86 (d, *J* = 8.0 Hz, 2H), 7.70 (d, *J* = 8.0 Hz, 2H), 7.59–7.53 (m, 1H), 7.48–7.31 (m, 2H); ^{13}C NMR ($CDCl_3$, 75 MHz): δ = 180.9, 163.1, 148.6, 143.6, 129.1, 126.8, 126.0, 125.9, 124.0, 123.2, 122.0, 122.2; HRMS: Calcd for $C_{17}H_{11}F_3N_2O$; Exact mass: 316.0823, found (ESI M+H) HRMS: *m* / *z* 317.0989 (M+H).

(*E*)-3-(4-(trifluoromethyl)phenyl)-1-(5-methyl-1*H*-benzo[*d*]imidazol-2-yl)prop-2-en-1-one (6j)

Yellow solid; 90 %; 222–224 °C; IR (cm^{-1}): 3279 (NH), 1661 (C=O), 1590 (C=C); ^{1}H NMR ($CDCl_3$, 400 MHz): δ = 10.28 (Broad s, 1H, NH), 8.18 (d, *J* = 16.0 Hz, 1H, –CH=CH–), 8.03 (d, *J* = 16.0 Hz, 1H, –CH=CH–), 7.86–7.84 (m, 3H), 7.70–7.68 (m, 4H), 253 (s, 3H, –CH_3); ^{13}C NMR ($CDCl_3$, 75 MHz): δ = 181.0, 140.2, 133.0, 132.3, 131.4, 129.7, 124.4, 122.9, 121.7, 120.6, 120.0, 116.2, 115.4, 115.0, 26.1; HRMS: Calcd for $C_{18}H_{13}F_3N_2O$; Exact mass: 330.0980, found (ESI M+H) HRMS: *m* / *z* 331.0887 (M+H).

(*E*)-1-(5-chloro-1*H*-benzo[*d*]imidazol-2-yl)-3-(4-(trifluoromethyl)phenyl)prop-2-en-1-one (6k)

Yellow solid; 94 %; 268–270 °C; IR (cm^{-1}): 3284 (NH), 1666 (C=O), 1602 (C=C); ^{1}H NMR ($CDCl_3$, 400 MHz): δ = 10.35 (Broad s, 1H, NH), 8.24 (d, *J* = 16.0 Hz, 1H, –CH=CH–), 8.10 (d, *J* = 16.0 Hz, 1H, –CH=CH–), 7.76–7.65 (m, 3H), 7.39–7.28 (m, 4H); ^{13}C NMR ($CDCl_3$, 75 MHz): δ = 181.8, 139.9, 135.2, 132.7, 132.0, 131.6, 126.1, 124.4, 124.0, 123.5, 122.5, 121.3, 118.7, 118.1, 115.5; HRMS: Calcd for $C_{17}H_{10}ClF_3N_2O$; Exact mass: 350.0434, found (ESI M+H) HRMS: *m* / *z* 351.0654 (M+H).

PROCEDURE OF THE SRB-ASSAY FOR ANTICANCER SCREENING

The human breast cancer cell line MCF-7 (procured from NCI, USA, and NCCS, Pune) was cultured in tissue culture flasks using RPMI-1640 medium supplemented with 2 mM L-glutamine (pH 7.4), 10 % fetal calf serum, 100 µg mL^{-1} streptomycin, and 100 U mL^{-1} penicillin. The cells were maintained at 37 °C in a humidified incubator under an atmosphere of 5 % CO_2. At the sub-confluent stage, cells were harvested by treatment with trypsin (0.05% in PBS containing 0.02 % EDTA) and resuspended in fresh growth medium. Only cell suspensions exhibiting viability greater than 97 %, as determined by the trypan blue exclusion method, were used for cytotoxicity studies. Approximately 5 × 10^3 cells in 100 µL of medium were seeded into each well of a 96-well tissue culture plate and allowed to adhere for 24 h at 37 °C. Test compounds at various concentrations were then added, and the plates were further incubated for 48 h under identical conditions. Appropriate blanks and positive controls were included, and all experiments were performed in triplicate. Following treatment, cell growth was terminated by the gentle addition of 50 µL of cold 50 % trichloroacetic acid (TCA) to each well, and the plates were incubated at 4 °C for 1 h to fix the cells. The supernatant was carefully removed, and the wells were washed five times with double-distilled water to eliminate residual medium and TCA, followed by complete air drying. The fixed cells were stained with 100 µL of 0.4 % sulforhodamine B (SRB) solution prepared in 1 % acetic acid and incubated at room temperature for 30 min. Excess unbound dye was removed by washing the wells five times with 1 % acetic acid, and the plates were air-dried. The protein-bound dye was subsequently solubilized by adding 100 µL of 0.01 M Tris buffer (pH 10.4) to each well, and the plates were gently agitated on a mechanical shaker for 5 min. Absorbance was measured at 540 nm using an ELISA plate reader. Cell growth in untreated control wells was taken as 100 %, and the percentage growth inhibition for each test compound was calculated accordingly. The GI_{50} values, defined as the concentration required to inhibit 50 % of cell growth, were determined by regression analysis.

RESULTS AND DISCUSSION

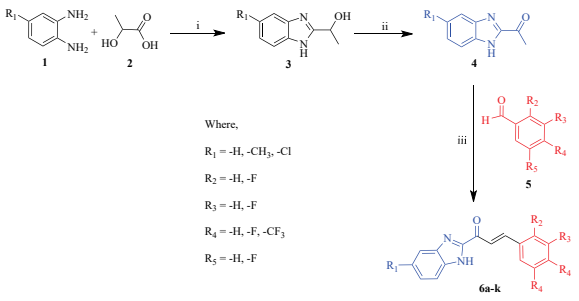
Chemistry

In the present study, a novel series of benzimidazole-chalcone derivatives (**6a–k**) was synthesized via base-catalyzed (KOH) aldol condensation of 2-acetylbenzimidazole **4** with various fluoro- or trifluoromethyl-substituted aromatic aldehydes **5** at 50–60 °C, affording the target compounds (Scheme 1). The key starting material, 2-acetylbenzimidazole **4**, was prepared through condensation of 4-methylbenzene-1,2-diamine or *o*-phenylenediamine **1** with lactic acid **2** in 4 N hydrochloric acid to generate the corresponding intermediate **3**. Subsequent oxidation of the hydroxyl group using potassium dichromate furnished 2-acetylbenzimidazole **4** in good yields (75–80 %, Scheme 1).[32] The crude products were purified by column chromatography and recrystallized from ethanol to afford benzimidazole chalcones. The structures of all synthesized compounds were unambiguously confirmed by FT-IR, ^{1}H NMR, ^{13}C NMR, and HRMS spectroscopic analyses. The α, β-unsaturated carbonyl system of chalcones typically exhibits a large vicinal coupling constant (J ≈ 12–16 Hz) between the olefinic protons (Hα and Hβ), which is indicative of an *E*-configuration. All synthesized benzimidazole-chalcones exhibited this diagnostic trans-coupling value.

Biological Evaluation

IN VITRO ANTICANCER ACTIVITY

The newly synthesized benzimidazole–chalcone derivatives (**6a–k**) were evaluated for their in vitro anticancer activity against the human breast cancer cell line MCF-7 and normal Vero cell line using the sulforhodamine B (SRB) assay method.[33] The MCF-7 cell line was chosen as the primary screening model owing to its well-characterized estrogen receptor–positive phenotype and its widespread use in preliminary cytotoxicity assessments of chalcone- and benzimidazole-based scaffolds. Furthermore, earlier studies[34] have reported that these structural classes exhibit preferential anticancer activity toward MCF-7 cells, underscoring the relevance of this model for initial biological evaluation.



Scheme 1. Reagents and conditions: (i) 4N HCl, Reflux, 2–3 h, 100 °C; (ii) $K_2Cr_2O_7/H_2SO_4$, 2.5 h at RT; (iii) KOH, PEG-300, 50-60 °C, 18 h.

During the screening, three key parameters GI_{50}, TGI, and LC_{50} were determined, and the results are summarized in Table 1, with adriamycin (ADR) used as the reference standard. The GI_{50} value represents the concentration of a compound required to inhibit cell growth by 50 % relative to untreated control cells, while TGI and LC_{50} correspond to the concentrations necessary for complete growth inhibition and for inducing 50 % cell death, respectively. On the basis of GI_{50} values, the compounds were classified according to their cytotoxic potency as inactive (>100 μM), moderately active (> 10 to <1 00 μM), and highly active (< 10 μM).

Overall, the synthesized compounds displayed a wide range of anticancer activities against MCF-7 cells, with GI_{50} values spanning from < 10 μM to > 100 μM. None of the compounds exhibited LC_{50} values below 100 μM, indicating that the derivatives predominantly exerted cytostatic rather than cytotoxic effects under the tested conditions. Only compound **6f** demonstrated measurable TGI activity (49.20 μM), while all other analogues showed TGI values > 100 μM.

Among the tested series, compounds **6a** (GI_{50} = 6.39 μM), **6b** (GI_{50} = 8.22 μM), and **6f** (GI_{50} = 3.66 μM) emerged as the most potent derivatives and were classified as highly active (GI_{50} < 10 μM). Notably, compound **6f** bearing fluoro substituents at both R_3 and R_5 positions exhibited the strongest growth inhibitory activity, suggesting a favorable role of fluorine substitution in enhancing anticancer potency. This compound also achieved partial growth arrest at higher concentrations, as evidenced by its TGI value.

Moderate anticancer activity (GI_{50} between 10 and 100 μM) was observed for compounds **6c**, **6d**, **6e**, **6g**, **6h**, **6i**, and **6k**. Among these, chloro- and methyl-substituted derivatives generally displayed reduced potency compared to fluoro-substituted analogues, indicating that electron-withdrawing fluorine atoms may contribute positively to activity by influencing lipophilicity and target interactions. In contrast, compounds incorporating trifluoromethyl substitution at the R_4 position (**6i–6k**) exhibited only moderate to weak activity, with GI_{50} values ranging from 23.93 to > 100 μM, suggesting that bulky CF_3 groups may adversely affect binding or cellular uptake.

Compound **6j**, containing both a methyl group and a trifluoromethyl substituent, was found to be inactive (GI_{50} > 100 μM), further supporting the notion that excessive steric bulk or suboptimal electronic distribution diminishes anticancer efficacy within this scaffold.

Although all synthesized compounds were less potent than the reference drug adriamycin (GI_{50} < 0.1 μM), several derivatives particularly **6f**, **6a**, and **6b** demonstrated

promising growth inhibitory activity, validating the benzimidazole–chalcone framework as a viable template for further optimization. The observed structure–activity relationship highlights the importance of strategic halogen substitution, especially fluorine, in modulating anticancer potency against estrogen receptor–positive breast cancer cells.

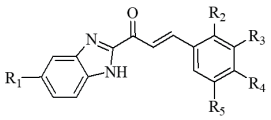
Overall, these findings provide valuable insights into the anticancer potential of benzimidazole chalcones and warrant further mechanistic studies and structural refinement to enhance their therapeutic efficacy.

The cytotoxicity profile of the synthesized benzimidazole–chalcone derivatives (**6a–k**) was additionally evaluated against the normal Vero cell line to assess their relative selectivity toward cancer cells. Most of the compounds showed relatively weak growth-inhibitory activity against Vero cells, with GI_{50} values > 100 μM for **6d–6g, 6i, 6j,** and **6k**. Compounds **6a, 6b, 6c,** and **6h** exhibited moderate activity, with GI_{50} values of 27.45, 20.27, 33.47, and 20.00 μM, respectively, while compound **6f** showed a GI_{50} of 31.30 μM and a TGI of 78.00 μM. In comparison, adriamycin exhibited a GI_{50} of 1.24 μM against Vero cells. Overall, the generally higher GI_{50} values observed for the synthesized compounds in Vero cells compared with MCF-7 cells, particularly for **6a, 6b,** and **6f**, suggest a degree of preferential growth inhibition toward MCF-7 cancer cells. These findings support the potential selectivity of selected derivatives and warrant further studies using additional normal cell lines and mechanistic assays to confirm their selectivity and safety profile.

Analysis of the anticancer data against MCF-7 cells reveals that both the nature and position of substituents on the aromatic rings of the benzimidazole–chalcone scaffold play a decisive role in modulating anticancer activity. Unsubstituted or lightly substituted analogues displayed appreciable activity, as exemplified by compound **6a** (GI_{50} = 6.39 μM). Introduction of a single fluoro substituent further enhanced potency, as observed for compound **6b** (GI_{50} = 8.22 μM), indicating that mild electron-withdrawing substitution is beneficial. The most potent derivative, **6f** (GI_{50} = 3.66 μM; TGI = 49.20 μM), bearing fluoro substituents at both R_3 and R_5 positions, highlights a synergistic effect of dual fluorination, possibly through optimized electronic distribution, improved lipophilicity, and enhanced interactions with the biological target.

In contrast, substitution with bulkier or less optimally positioned groups resulted in diminished activity.

Table 1. *In vitro* anticancer screening of benzimidazole chalcones (**6a–k**) against human breast cancer cell line MCF-7[(a)] and normal Vero cell line.



Compound	R_1	R_2	R_3	R_4	R_5	MCF-7			Vero		
						LC_{50}[(b)]	TGI[(c)]	GI_{50}[(d)]	LC_{50}[(b)]	TGI[(c)]	GI_{50}[(d)]
6a	H	H	H	H	H	>100	>100	6.39	>100	72.43	27.45
6b	H	F	H	H	H	>100	>100	8.22	>100	>100	20.27
6c	H	F	H	F	H	>100	>100	15.21	>100	>100	33.47
6d	CH_3	H	H	F	H	>100	>100	14.33	>100	>100	>100
6e	Cl	H	H	F	H	>100	>100	83.30	>100	>100	>100
6f	H	H	F	H	F	>100	49.20	3.66	>100	78.00	31.30
6g	CH_3	H	F	H	F	>100	>100	21.89	>100	>100	>100
6h	Cl	H	F	H	F	>100	>100	13.97	>100	>100	20.00
6i	H	H	H	CF_3	H	>100	>100	30.66	>100	>100	>100
6j	CH_3	H	H	CF_3	H	>100	>100	>100	>100	>100	>100
6k	Cl	H	H	CF_3	H	>100	>100	23.93	>100	>100	>100
ADR[(e)]		37.18	1.65	<0.1	>100	10.0	1.24				

[(a)] Concentrations in μM.

[(b)] Concentration of drug resulting in a 50 % reduction in the measured protein at the end of the drug treatment as compared to that at the beginning) calculated from $[(Ti - Tz)/Tz] \times 100 = -50$.

[(c)] Drug concentration resulting in total growth inhibition (TGI) will calculated from $Ti = Tz$.

[(d)] Growth inhibition of 50 % (GI_{50}) calculated from $[(Ti - Tz)/(C - Tz)] \times 100 = 50$.

[(e)] ADR = Adriamycin.

Chloro- and methyl-substituted analogues **(6c-6e, 6g, 6h)** exhibited only moderate growth inhibition (GI_{50} = 13.97–83.30 µM), suggesting that increased steric demand or altered electronic effects at these positions are less favorable for anticancer efficacy. Notably, derivatives incorporating a trifluoromethyl group at the R_4 position **(6i–6k)** showed moderate to weak activity (GI_{50} = 23.93 to > 100 µM), while compound **6j** was completely inactive, implying that excessive steric bulk and strong electron-withdrawing character of the CF_3 group may hinder effective target binding or cellular uptake. Collectively, the structure activity relationship (SAR) trends indicate that judicious incorporation of fluorine atoms, particularly at multiple positions, enhances anticancer potency, whereas bulky substituents such as CF_3 negatively impact activity within this benzimidazole–chalcone framework.

The observed anticancer activity of the benzimidazole–chalcone derivatives may be associated with mechanisms reported for these scaffolds, including induction of apoptosis and modulation of cell-cycle progression.[35,36] Chalcones have been reported to induce cell-cycle arrest and apoptosis through modulation of cyclins, cyclin-dependent kinases, tubulin, and apoptotic signaling pathways, while benzimidazole derivatives have also been associated with apoptosis induction and G2/M cell-cycle arrest.[35,36] The higher activity observed for **6a, 6b,** and particularly **6f** may therefore reflect favorable interactions with cellular targets involved in proliferation and survival. The enhanced activity of fluorinated derivative **6f** may also be related to favorable electronic and physicochemical properties; however, this interpretation remains speculative. Since apoptosis and cell-cycle pathways were not directly investigated in the present SRB assay, further studies are required to establish the precise mechanism of action.[37]

CONCLUSION

In conclusion, a new series of benzimidazole–chalcone derivatives (**6a**–**k**) was efficiently synthesized and structurally confirmed by spectroscopic analyses, with all compounds exhibiting the characteristic trans (*E*)-configured α, β-unsaturated carbonyl system. *In vitro* evaluation against MCF-7 breast cancer cells identified several active derivatives, particularly fluoro-substituted analogues, with the difluoro compound **6f** showing the most potent growth inhibitory activity. Evaluation against normal Vero cells showed generally weaker growth inhibition for several derivatives, indicating preliminary differential activity toward MCF-7 cells. Structure–activity relationship analysis highlighted the influence of substituent type and position, with fluorine substitution associated with enhanced anticancer activity, whereas bulky trifluoromethyl groups generally reduced activity. Although less potent than adriamycin, the observed growth-inhibitory effects and preliminary selectivity profile support the benzimidazole–chalcone scaffold for further structural optimization and mechanistic investigation toward the development of improved anticancer candidates.

Acknowledgment. The authors gratefully acknowledge the Tata Memorial Centre, Advanced Centre for Treatment, Research and Education in Cancer (ACTREC), Kharghar, Navi Mumbai–410210, for carrying out the *in vitro* anticancer screening studies.

Supplementary Information. Supporting information to the paper is attached to the electronic version of the article at: https://doi.org/10.5562/cca4375.

PDF files with attached documents are best viewed with Adobe Acrobat Reader which is free and can be downloaded from Adobe's web site.

REFERENCES

[1] World Health Organization. *Global Cancer Statistics 2020*. WHO, Geneva, **2021**.

[2] F. Bray, J. Ferlay, I. Soerjomataram, R. L. Siegel, L. A. Torre, A. Jemal, *CA-Cancer J. Clin.* **2018**, *68*, 394–424. https://doi.org/10.3322/caac.21492

[3] H. Sung, J. Ferlay, R. L. Siegel, M. Laversanne, I. Soerjomataram, A. Jemal, F. Bray, *CA-Cancer J. Clin.* **2021**, *71*, 209–249. https://doi.org/10.3322/caac.21660

[4] F. Bray, M. Laversanne, H. Sung, J. Ferlay, R. L. Siegel, I. Soerjomataram, A. Jemal, *CA-Cancer J. Clin*. **2024**, *74*, 229–263. https://doi.org/10.3322/caac.21834

[5] A. Waks, E. Winer, *JAMA* **2019**, *321*, 288–300. https://doi.org/10.1001/jama.2018.19323

[6] N. Harbeck, F. P. Llorca, J. Cortes, M. Gnant, N. Houssami, P. Poortmans, K. Ruddy, J. Tsang, F. Cardoso, *Nat. Rev. Dis. Primers*, **2019**, *5*, 66. https://doi.org/10.1038/s41572-019-0111-2

[7] N. Mahurkar, N. Gawhale, M. Lokhande, S. Uke, M. Kodape, *Results Chem.* **2023**, *6*, 101139. https://doi.org/10.1016/j.rechem.2023.101139

[8] M. Pitucha, M. Janeczko, K. Klimek, E. Fornal, M. Wos, A. Pachuta-Stec, G. Ginalska, A. Kaczor, *Bioorg. Chem.* **2020**, *99*, 103806. https://doi.org/10.1016/j.bioorg.2020.103806

[9] M. Tuncbilek, T. Kiper, N. Altanlar, N. *Eur. J. Med. Chem*. **2009**, *44*, 1024–1033. https://doi.org/10.1016/j.ejmech.2008.06.026

[10] R. Shingalapur, K. Hosamani, R. Keri, *Eur. J. Med. Chem*. **2009**, *44*, 4244–4248. https://doi.org/10.1016/j.ejmech.2009.05.021

[11] G. Surineni, Y. Gao, M. Hussain, Z. Liu, Z. Lu, C. Chhotaray, M. Islam, H. Hameed, T. Zhang, *Med. Chem. Commun*. **2019**,*10*, 49–60. https://doi.org/10.1039/C8MD00389K

[12] H. Zhang, G. Damu, G. Cai, C. Zhou, *Eur. J. Med. Chem*. **2013**, *64*, 329–344. https://doi.org/10.1016/j.ejmech.2013.03.049

[13] F. Hernandez-Luis, A. Hernandez-Campos, R. Castillo, G. Navarrete-Vazquez, O. Soria-Arteche, M. Hernandez-Hernandez, L. Yepez-Mulia, *Eur. J. Med. Chem*. **2010**, *45*, 3135–3141. https://doi.org/10.1016/j.ejmech.2010.03.050

[14] D. Valdez-Padilla, S. Rodriguez-Morales, A. Hernandez-Campos, F. Hernandez-Luis, L. Yepez-Mulia, A. Tapia-Contreras, R. Castillo, *Bioorg. Med. Chem*. **2009**, *17*, 1724–1730. https://doi.org/10.1016/j.bmc.2008.12.059

[15] S. Rida, S. El-Hawash, H. Fahmy, A. Hazzaa, M. El-Meligy, *Arch Pharm Res*. **2006**, *29*, 826–833. https://doi.org/10.1007/BF02973901

[16] Y. Luo, J. Yao, L. Yang, C. Feng, W. Tang, G. Wang, J. Zuo, W. Lu, *Bioorg. Med. Chem*. **2010**, *18*, 5048–5055. https://doi.org/10.1016/j.bmc.2010.05.076

[17] P. Singla, V. Luxami, K. Paul, *RSC Adv.* **2014**, *4*, 12422–12440. https://doi.org/10.1039/C3RA46304D

[18] Y. Lee, Y. Tan, C. Oon, *Acta Pharm. Sin. B.*, **2023**, *13*, 478–497. https://doi.org/10.1016/j.apsb.2022.09.010

[19] Y. Bansal, O. Silakari, *Bioorg. Med. Chem.* **2012**, *20*, 6208–6236. https://doi.org/10.1016/j.bmc.2012.09.013

[20] Z. Nowakowska, *Eur. J. Med. Chem.* **2007**, *42*, 125–137. https://doi.org/10.1016/j.ejmech.2006.09.019

[21] C. Zhuang, W. Zhang, C. Sheng, W. Zhang, C. Xing, Z. Miao, *Chem. Rev.* **2017**, *117*, 7762–7810. https://doi.org/10.1021/acs.chemrev.7b00020

[22] B. Narasimhan, A. Sapra, *Lett. Drug Des. Discov*. **2025**, *22*, 100237. https://doi.org/10.1016/j.lddd.2025.100237

[23] M. A. S Badawy, S. Bräse, T. F. S. Ali, M. Abdel-Aziz, H. Abdel-Rahman, *Pharmaceuticals,* **2025**, *18*, 1454. https://doi.org/10.3390/ph18101454

[24] Keri, R. S.; et al. Hybrid molecules in anticancer drug design. *Eur. J. Med. Chem.* **2018**, 147, 268–299.

[25] F. Hagar, S. Abbas, H. Gomaa, B. Youssif, A. Sayed, D. Abdelhamid, M. Abdel-Aziz, *BMC chemistry* **2023**, *17*, 116. https://doi.org/10.1186/s13065-023-01003-3

[26] S. Tahlan , S. Singh , K. Pandey, K. Singh, *Mini Rev. Med. Chem*. **2025**, *25*, 440–462. http://dx.doi.org/10.2174/0113895575329633240928163509

[27] S. Dongare, B. Bandgar, P. Bhale, S. Shringare, H. Chavan, *Croat. Chem. Acta.* **2019**, *92*, 1–9. https://doi.org/10.5562/cca3418

[28] P. Bhale, H. Chavan, S. Shringare, V. Khedkar, R. Tigote, N. Mali, T. Jadhav, N. Kamble, S. Kolat, B. Bandgar, H. Patil, *Synth. Commun*. **2022**, *52*, 733–744. https://doi.org/10.1080/00397911.2022.2048860

[29] P. Bhale, S. Shringare, A. Khade, H. Chavan, *Anti-Cancer Agents Med. Chem.* **2021**, *21*, 2216–2223. https://doi.org/10.2174/1871520621666210201095030

[30] P. Bhale, H. Chavan, R. Endait, A. Kadam, R. Bopalkar, M. Gaikwad, *Croat. Chem. Acta.* **2021**, *94*, 35–41. https://doi.org/10.5562/cca3758

[31] P. Bhale, H. Chavan, S. Dongare, S. Sankpal, B. Bandgar, *Anti-Cancer Agents Med. Chem.* **2018**, *18*, 757–764. https://doi.org/10.2174/1871520617666170912124258

[32] M. Phillips, *J. Chem. Soc*., **1928**, *131*, 2393–2399. https://doi.org/10.1039/JR9280002393

[33] P. Skehan, R. Strong, D. Scadiaro, A. Monks, J. McMahon, D. Vistica, J. Warren, H. Bokesch, S. Kenney, M. Boyed, *J. Natl. Cancer Inst.* **1990**, *82*, 1107–1112. https://doi.org/10.1093/jnci/82.13.1107

[34] V. Sundharaj, V. Vijayakumar, S. Sarveswari, *Results Chem.* **2026**, *21*, 103042. https://doi.org/10.1016/j.rechem.2026.103042

[35] Y. Ouyang, J. Li, X. Chen, X. Fu, S. Sun, Q. Wu, *Biomolecules* **2021**, *11*, 894. https://doi.org/10.3390/biom11060894

[36] L. Feng, W. Su, J. Cheng, T. Xiao, H. Li, D. Chen, Z. Zhang, *Archiv der Pharmazie* **2022**, 355, e2200051. https://doi.org/10.1002/ardp.202200051

[37] H. Atmaca, S. İlhan, M. Batır, Ç. Pulat, A. Güner, H. Bektaş, *Chemico-Biological Interactions* **2020**, 327, 109163. https://doi.org/10.1016/j.cbi.2020.109163